2010

High-Pressure and High-Temperature Density Measurements of n-Pentane, n-Octane, 2,2,4-Trimethylpentane, Cyclooctane, n-Decane, and Toluene

Yue Wu
Virginia Commonwealth University

High-Pressure and High-Temperature Density Measurements of n-Pentane, n-Octane, 2,2,4-Trimethylpentane, Cyclooctane, n-Decane, and Toluene

A thesis submitted in partial fulfillment of the requirements for the degree of Master of Science at Virginia Commonwealth University.

by

Yue Wu,
Master of Science,
Virginia Commonwealth University, 2010

Director: Mark A. M^{c}Hugh,
Professor, Department of Chemical and Life Science Engineering

Virginia Commonwealth University
Richmond, Virginia
October, 2010

Acknowledgment

I thank my advisor, Professor Mark A. M^{c}Hugh for his guidance over the years. He will always be given my respect for guiding me through the ocean of chemical engineering. His devotion to the science, great personality, and sense of humor impress me a lot. I do enjoy working in Professor McHugh's Lab.

I acknowledge Dr. Kun Liu for helping me get familiar with the high-pressure view cell system and some density experiments.

I thank my family and girlfriend for their support throughout my life. I wish all of them health and happiness.

Table of Contents

List of Tables

List of Figures

Abstract

HIGH-PRESSURE AND HIGH-TEMPERATURE DENSITY MEASUREMENT OF N-PENTANE, N-OCTANE, 2,2,4-TRIMETHYLPENTANE, CYCLOOCTANE, N-DECANE, AND TOLUENE

By Yue Wu, M.S.

A thesis submitted in partial fulfillment of the requirements for the degree of Master of Science at Virginia Commonwealth University.

Virginia Commonwealth University, 2010.

Major Director: Mark A. M^{c}Hugh, Professor, Department of Chemical and Life Science Engineering

Information on the density of hydrocarbons at high pressures and temperatures is of great importance in many fields, such as the study of ultra-deep reservoirs up to ~240 MPa and 250°C. However, density data at such high pressures and temperatures are often not available in the literature. In this study, experimental densities are reported for n-pentane, n-octane, 2,2,4-trimethylpentane, cyclooctane, n-decane, and toluene to ~280 MPa and ~250°C. These experimental densities are in good agreement with available literature data, although the literature data for many of these fluids do not extend to the pressures and temperatures utilized in this study.

Chapter 1 Introduction

In the field of petroleum engineering, density information of hydrocarbons at high pressure and temperature conditions is a basis for both mass and volumetric flow rate determination, which leads to a determination of solution viscosity. Hydrocarbon density predictions and data at extreme pressures and temperatures are needed for the characterization of the oils in ultra-deep reservoirs [1, 2]. At ultra-deep reservoir depth of 4,600 meters or more, crude oils containing high sulfur contents have very high densities. The goal of this research is to develop and apply a reliable experiment technique to measure the density of different hydrocarbons at temperatures to 250°C and pressures to 280 MPa.

To our best knowledge, there are mainly three methods used for measuring high-pressure, high-temperature densities measurement: vibrating-wire, bellows volumometer, and floating piston. The vibrating-wire system takes the advantage of the buoyancy force exerted on the sinker and detects the force with a vibrating wire inside the cell. The tension of the wire can be related to its resonant frequency with a complete theoretical analysis, leading to a value for the density as well as the viscosity of the fluid surrounding the wire [3-7]. This technique is highly valued by simultaneously measuring the density and viscosity of the working fluid and not requiring an

extensive calibration procedure, while it is relatively complicated both for the theoretical calculations need to analyze the data and the sensitivity of the apparatus that is used. The bellow volumometer operates by the principle that the length of the bellows changes with the applied pressure. The bellows can be extended under vacuum and it can be compressed when subject to an external pressure. At a given pressure, the change of volume is obtained by measuring the change of length of the bellows by some instrument, such as a linear variable differential transformer (LVDT) and, hence, the density of the fluid inside the bellows can be calculated [8]. The floating piston apparatus also uses volume displacement information to determine densities, either by fixing the temperature and continuously changing the volume and pressure [9-11], or by keeping the volume fixed and changing the pressure and temperature [12-14]. Unlike the bellows system, the floating piston technique uses a piston with a special o-ring to separate the testing fluid from the hydraulic fluid. It should be noted that for both a bellows and a piston, a separate internal cell volume calibration is always required by correlating the volume to the LVDT reading before any density determination experiment. Besides these three density measurement techniques, there are a few other approaches found in the literature, such as a resonance densimeter [15-19], which is usually combined with a viscometer for the measurement of viscosity [16, 18, 19]. However, the main drawback with this technique is the operating pressure is limited to 100 MPa and, hence, not a common technique used for the high-pressure density measurements.

In this study, the floating piston technique is employed. However, rather than fix the piston in a specific position in the cell and change the temperature and pressure, the piston is moved to change the volume in the cell. The piston location is determined with an LVDT. Since the amount of the testing liquid is known, the density can be calculated by dividing the liquid mass

by the internal volume at a fixed temperature and pressure. This system benefits from its simplicity and straightforward operation at high pressures and temperatures, while the main disadvantage of this system is that o-rings are used for pressure sealing and for separating the fluid of interest from the hydraulic fluid used to move the piston. O-rings can fail at high temperatures and they can swell in certain fluids. Hence, careful selection of the o-rings is needed for the best performance.

The goal of this study is to expand the current density database for single component hydrocarbon constituents that can be found in petroleum fluids. The hydrocarbons of interest include n-pentane, n-octane, n-decane, 2,2,4-trimethylpentane, cyclooctane, and toluene. Table 1 lists the literature references for densities of n-pentane, n-octane, 2,2,4-trimethylpentane, n-decane, and toluene at high pressures and temperatures. The table also lists the number of data points and the temperature and pressure range for each literature reference. As seen from the table, there are some densities at relatively high pressures [9, 20-25] or temperatures [26-28], however, there are no alkane density data at both high pressures up to 280 MPa and temperatures up to 250°C.

In the following chapter, details are given on the experimental technique used to obtain densities at pressures to 280 MPa and temperatures to 250°C. Chapter 3 reports and analyzes the experimental density data of n-pentane, n-octane, 2,2,4-trimethylpentane, n-decane, and toluene at high pressures and temperatures. Chapter 4 lists the conclusions and future work recommended from this study. It should be noted that the pressure gauge used in the present study has units of psi rather than the international system of unit (SI unit) for pressure, MPa, so

in Chapter 2 the pressure is reported in psi units and is converted to MPa in certain cases. The data reported in Chapter 3 are in MPa units for ease of comparison to the literature data.

Table 1. Literature references of high-pressure density measurement for n-pentane, n-octane, 2,2,4-trimethylpentane, n-decane, and toluene.

Reference	# of Data Points	Pressure (MPa) Min	Pressure (MPa) Max	Temperature (°C) Min	Temperature (°C) Max	Method
			n-Pentane			
Bridgman (1931)[20]	30	98.1	981	0	95	Bellows
Byun (2000)[9]	84	7.0	241	50	150	Floating Piston
Easteal (1987)[29]	35	0.1	60	5	65	Bellows
Audonnet (2001)[4]	40	0.1	100	30	110	Vibrating-wire
Oliveira (1992)[23]	29	0.1	252	30	50	Vibrating-wire
Palavra (1987)[21]	68	1.8	283	33	69	Vibrating-wire
Kiran (1992)[10]	139	7.5	70	45	170	Floating Piston
Kiran (1996)[30]	52	8.1	65	75	150	Floating Piston
			n-Octane			
Bridgman (1931)[20]	22	49.0	981	0	95	Bellows
Harris (1997)[22]	61	0.1	373	10	80	Bellows
Caudwell (2009)[28]	67	0.1	202	25	200	Vibrating-wire
Oliveira (1992)[23]	48	0.1	253	30	75	Vibrating-wire
Kiran (1992)[10]	47	8.0	66	50	175	Floating Piston
Moravkova (2006)[15]	92	0.1	40	25	55	Resonance Densimeter
Dymond (1982)[25]	28	0.1	480	25	75	Bellows
			2,2,4-Trimethylpentane			
Malhotra (1990)[31]	8	49.0	588	5	65	Bellows
Malhotra (1993)[24]	89	0.1	374	40	80	Bellows
Padua (1994)[32]	33	0.1	100	25	75	Vibrating-wire
Padua (1996)[5]	85	0.1	100	-75	75	Vibrating-wire
			n-Decane			
Bridgman (1931)[20]	17	49.0	785	0	95	Bellows
Audonnet (2004)[33]	40	0.1	76	30	120	Vibrating-wire
Caudwell (2009)[28]	19	0.1	192	25	100	Vibrating-wire
Oliveira (1992)[23]	46	0.1	254	30	75	Vibrating-wire
Dymond (1982)[25]	19	0.1	420	25	100	Bellows

Reference	# of Data Points	Pressure (MPa) Min	Pressure (MPa) Max	Temperature (°C) Min	Temperature (°C) Max	Method
			Toluene			
Harris (1997)[22]	22	0.1	373	25	50	Bellows
Oliveira (1992)[23]	46	0.1	252	30	75	Vibrating-wire
Assael (1991)[34]	30	0.1	71	30	50	Vibrating-wire
Et-Tahir (1995)[16]	45	0.1	40	25	90	Resonance Densimeter
Glen (2009)[35]	73	0.6	30	20	100	Floating Piston
Dymond (1995)[36]	23	0.1	492	25	50	Bellows
Polhler (1996)[11]	69	3.4	65	50	150	Floating Piston
Franck (1998)[13]	117	5.0	300	50	400	Floating Piston

Chapter 2 Experimental Methods

2.1 Apparatus for High-pressure Density Measurements

The experimental system is illustrated in Figure 1, which consists of a high-pressure view cell, linear variable transformer (LVDT), pressure transducer, temperature control and measurement system, display system, and thermoset insulation. The schematic diagram of the view cell and LVDT is shown in Figure 2. A cylindrical view cell, constructed of a high nickel content steel (Nitronic 50^{TM}), is 7.00 cm outside diameter, 1.59 cm inside diameter, and approximately 35 ml working volume. A 1.9 cm outside diameter by 1.9 cm thick sapphire window is fitted to one end of the cell. The window is sealed by a 116 viton o-ring (15/16" O.D., 3/4" I.D.) and a 116 EPR backup o-ring. After securing the window in the cell, the end cap is bolted to the cell body. The cell is flipped vertically and a stir bar is loaded in the cell followed by the piston. For the piston, a 205 viton o-ring (11/16" O.D., 7/16" I.D.) is used to separate the cell contents from water, which is the hydraulic fluid used to move the piston. Then a rod with a magnetic end piece, called a core, is connected to the other side of the piston. The core travels through an LVDT (Schaevitz Corp., Model 2000 HR) to measure the change of the internal cell volume due to the displacement of the piston. A type-K thermocouple (Omega Corporation) connected to one of the

side ports is used to measure the temperature of the fluid in the view cell, which is housed in an air bath. The cell is also wrapped with heating bands to obtain very high operating temperatures. The typical control of the temperature of the air bath and heating bands is ± 0.2°C. After loading the fluid of interest into the cell through the other side port, the water is pressurized by the high-pressure generator (HIP Inc., model 37-5.75-60), pushing the piston forward to compress the fluid of interest. The system pressure is measured by a calibrated pressure transducer (Viatran Corporation, Model 245, 0 - 50,000 psig (345 MPa), accurate to ± 50 psig (0.35 MPa)) on the water side of the piston.

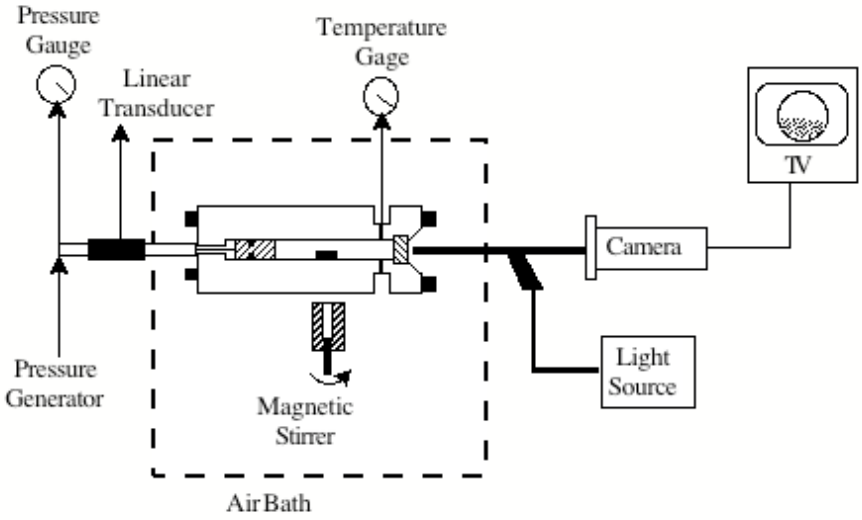

Figure 1. Schematic diagram of the experimental system used in this study to obtain high-pressure density measurements.

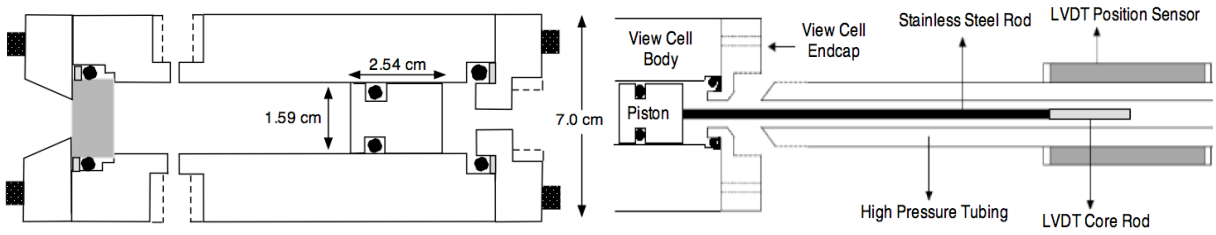

(A) (B)

Figure 2. Schematic diagram of (A) the high-pressure view cell used in this study, and (B) the LVDT used for volume measurements.

2.2 Calibration of the Pressure Transducer, Thermocouple, and Cell Internal Volume

2.2.1 Pressure Transducer Calibration

The transducer used to determine the pressure in the view cell is calibrated against a Heise pressure gauge (Heise Corporation, Model CC, 0 - 10,000 psig (68.9 MPa)), accurate to ± 10 psig (0.07 MPa) for pressures below 10,000 psig and an identical Viatran-calibrated pressure transducer (Viatran Corporation, Model 245, 0 - 50,000 psig (345 MPa)), accurate to ± 50 psig (0.35 MPa), is used to measure pressures from 10,000 to 40,000 psig. Since the pressure transducer is on the water side of the piston and will be always used at room temperature during the experiment, the pressure calibration experiments are performed at room temperature.

Table 2 and Table 3 show the results of pressure transducer calibration against the Heise pressure gauge up to 10,000 psig (68.0 MPa) and the Viatran-calibrated pressure transducer up to 30,000 psig (~200 MPa). The readings from the pressure transducer used in the experiment, $P_{view\ cell}$, are

in good agreement with the pressure readings from the Heise gauge, P_{Heise}, and the readings from the Viatran-calibrated pressure transducer, $P_{Viatran}$, below 8,200 psig (55.8 MPa). $P_{view\ cell}$ is always a little bit larger than P_{Heise} and $P_{Viatran}$ at pressures greater than 8,200 psig. Therefore, the view cell pressure transducer readings are accurate up to 8,200 psig without any correction and when pressure is greater than 8,200 psig, a calibration equation is used.

Table 2. Comparison of the pressure measurements from the pressure transducer used in this study ($P_{view\ cell}$) against the measurements using the Heise pressure gauge (P_{Heise}) and Viatran-calibrated pressure transducer ($P_{Viatran}$) at room temperature and pressures up to 10,000 psig (68 MPa).

P_{Heise} (psig)	$P_{Viatran}$ (psig)	$P_{view\ cell}$ (psig)	$\Delta P_1 = P_{Heise} - P_{view\ cell}$ (psig)	$\Delta P_2 = P_{Viatran} - P_{view\ cell}$ (psig)	$\Delta P_1 - \Delta P_2$ (psig)
500	495	490	10	5	5
990	975	980	10	-5	15
1480	1470	1470	10	0	10
1980	1975	1970	10	5	5
2470	2465	2460	10	5	5
2990	2980	2980	10	0	10
3500	3505	3500	0	5	-5
4000	4005	4000	0	5	-5
4500	4495	4500	0	-5	5
4970	4965	4970	0	-5	5
6250	6240	6250	0	-10	10
7200	7195	7210	-10	-15	5
8188	8165	8200	-12	-35	23
9275	9255	9300	-25	-45	20

Table 3. Comparison of the pressure measurements from the calibration of pressure transducer used in this study ($P_{view\ cell}$) against the measurements using the Viatran-calibrated pressure transducer ($P_{Viatran}$) at room temperature and pressures up to 30,000 psig (~200 MPa).

$P_{Viatran}$ (psig)	$P_{view\ cell}$ (psig)	$\Delta P = P_{Viatran} - P_{view\ cell}$ (psig)
770	760	10
1635	1620	15
2390	2380	10
3285	3280	5
4525	4520	5
5850	5850	0
7280	7290	-10
9110	9160	-50
10445	10500	-55
12070	12140	-70
13570	13650	-80
14915	15020	-105
16995	17120	-125
19115	19270	-155
20890	21070	-180
23050	23270	-220
24815	25070	-255
26830	27120	-290
29775	30130	-355

Figure 3 compares the reading from the view cell pressure transducer with the Viatran-calibrated pressure transducer. According to the figure, at pressure greater than 8,200 psig (55.8 MPa), a pressure calibration equation is obtained as

$$P_{correct}\,(\text{psig}) = 0.985 \bullet P_{view\ cell}\,(\text{psig}) + 123 \qquad \text{for } P > 8{,}200 \text{ psig} \qquad (1)$$

Since the view cell pressure transducer is within ±10 psig (0.07 MPa) of the Heise gauge when pressure is below 8,200 psig (55.8 MPa), the transducer is considered accurate to ±10 psig (0.07 MPa) when pressure is below 8,200 psig and ±50 psig (0.34 MPa) for pressure from 8,200 to 30,000 psig. Note that σ_{slope} and $\sigma_{intercept}$ refer to the uncertainties of slope and intercept of the pressure calibration curve, respectively. The small value of the uncertainties of the slope indicates the accuracy of the slope of the calibration curve. $\sigma_{intercept}$ is not taken seriously, since the calibration equation only works at pressure above 8,200 psi and will not be extended to the pressure of zero. The error bars are also plotted for readings from both the view cell pressure transducer and the Viatran-calibrated pressure transducer, but they are much smaller than the size of the data points and cannot be seen in the figure.

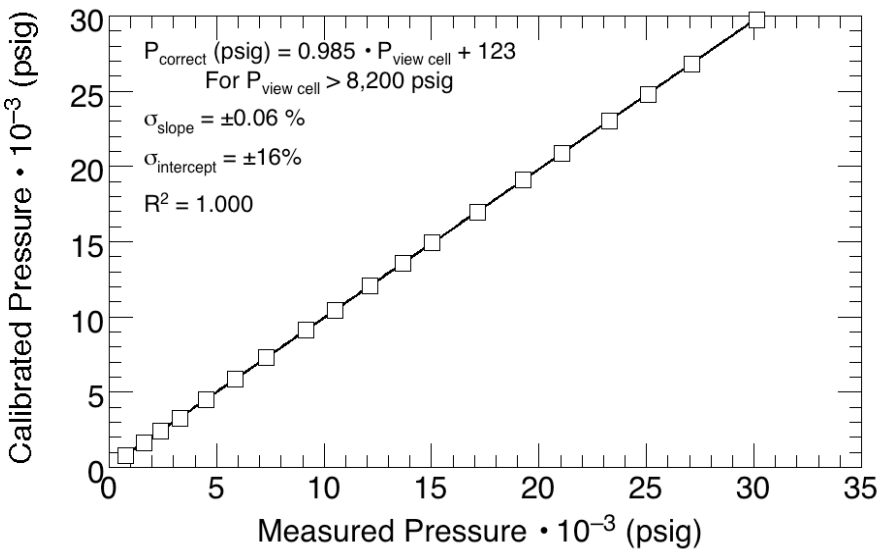

Figure 3. Calibration curve of the pressure transducer used in this study. σ_{slope} and $\sigma_{intercept}$ are the uncertainties of the fit of curve to the calibration data.

2.2.2 Thermocouple Calibration

The type-K thermocouple, $T_{Type\text{-}K}$, is calibrated against a precision immersion thermometer, T_{Hg}, (Fisher Scientific, 35 to 200°C, precise to 0.1°C, accurate to better than ± 0.10°C, recalibrated by ThermoFisher Scientific Company at four different temperatures using methods traceable to NIST standards) using a temperature-controlled silicone oil bath (Dow Company, Syltherm 800, recommended for –20°C to 200°C) at atmosphere pressure. The results from the thermocouple calibration are shown in Table 4 and the equation of temperature correction, obtained from Figure 4, is

$$T_{correct}\ (°C) = 0.992 \bullet T_{Type\text{-}k}\ (°C) - 0.285 \qquad (2)$$

Table 4. Comparison of the temperature measurements from the type-K thermocouple used in this study against the measurements of the calibrated immersion thermometer, T_{Hg}, at atmosphere pressure.

T_{Hg} (°C)	$T_{Type\text{-}K}$ (°C)
50.25	50.90
101.20	102.10
124.85	126.55
150.10	151.30

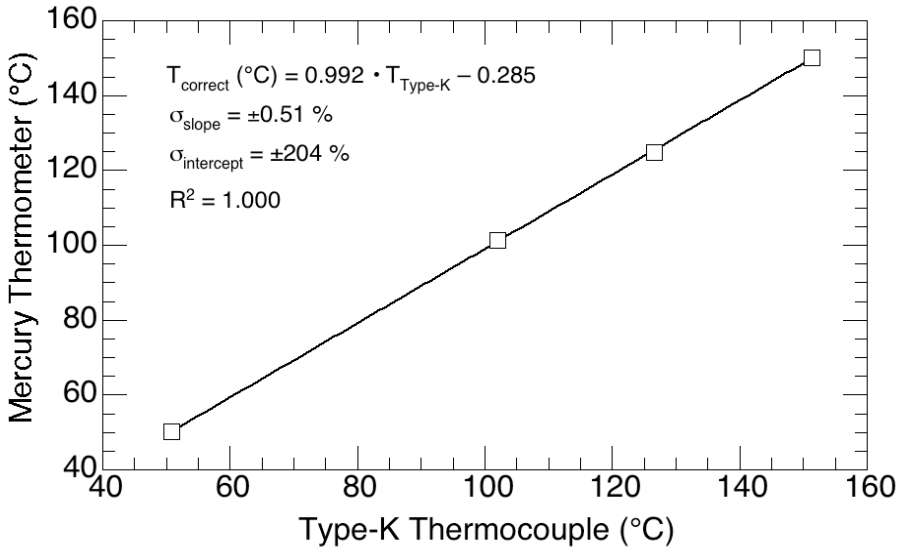

Figure 4. Calibration curve of the type-K thermocouple used in this study. σ_{slope} and $\sigma_{intercept}$ are the uncertainties of the fit of curve to the calibration data.

Note that σ_{slope} and $\sigma_{intercept}$ refer to the uncertainties of slope and intercept of the temperature calibration curve, respectively. The small value of the uncertainties of the slope indicates the accuracy of the slope of the calibration curve. $\sigma_{intercept}$ is not taken seriously, since the calibration equation only works at temperatures greater than 45 °C and will not be extended to the temperature of 0°C. The error bars are also plotted for readings from both the thermocouple and

the calibrated thermometer, but they are much smaller than the size of the data points and cannot be seen in the figure.

2.2.3 Cell Internal Volume Calibration

The internal cell volume is calibrated against the LVDT reading with pure n-decane (99.0% purity) at 50, 150 and 250°C. Before an experiment, the cell is flushed three times with ethane at room temperature and a pressure of ~150 psig (1.0 MPa) to remove any air trapped in the cell. Table 5 provides estimates of the amount of air and ethane that remains in the cell after each flushing at room temperature, where "charge" and "degas" refer to charging ethane into the cell and degassing it out of the cell. Since the pressure inside the cell is always below 150 psig, the ideal gas law is used to determine total amount of air remaining in the cell. The air and ethane are assumed to be well mixed for each charging step, so the amount of air that remains in the cell for each degassing process can be obtained by multiplying the mass of the gas mixture after degassing by the weight percent of air in the total gas before degassing. For the calculation shown in Table 5, it is assumed that eight grams of a hydrocarbon is loaded into the cell. Hence, the weight percent of either air or ethane in the hydrocarbon can be calculated. The results in Table 5 show that after flushing with ethane three times, the air remaining in the cell is approximately a 0.0002 wt% in the hydrocarbon and the weight percent of ethane is a 0.2 wt% in the hydrocarbon. These low amounts of air and ethane are not expected to have a significant influence on the reported density measurement.

Table 5. The amount of air and ethane remaining in the high-pressure view cell after each flushing with ethane at room temperature (21.7°C). Here it is assumed that eight grams of hydrocarbon liquid is loaded into the cell.

Step	P (psia)	Volume (ml)	Total Gas (Air + Ethane) (g)	Air (g)	wt% Air in Gas	wt% Air in Hydrocarbon	wt% Ethane in Hydrocarbon
Initial	15	14.0	0.017	0.017	100.00	0.207	0
1st Charge	145	15.6	0.183	0.017	9.05	0.202	2.03
1st Degas	15	14.4	0.018	0.002	9.05	0.020	0.20
2nd Charge	135	15.6	0.173	0.002	0.92	0.020	2.10
2nd Degas	15	14.4	0.018	0.0002	0.92	0.002	0.22
3rd Charge	135	15.6	0.174	0.0002	0.09	0.002	2.12
3rd Degas	15	12.4	0.015	0.00001	0.09	0.0002	0.19

A 10 mL syringe is used to load 7.0 to 9.0 ± 0.001 grams of n-decane through the top port of the cell. The exact mass of the loaded fluid is calculated by subtracting the mass of the syringe and n-decane before loading from the mass of the syringe and fluid after loading, both of which are weighed by a scale accurate to 0.0001 gram. The amount of air that goes into the cell is ignored during this process. The temperature is increased and stabilized at around 50°C followed by increasing the pressure in the cell up to ~40,000 psig. The LVDT readings are recorded at around 4,000 psig (27.2 MPa), 8,000 psig (54.4 MPa), 12,000 psig (81.6 MPa), 16,000 psig (108.8 MPa), 20,000 psig (136.1 MPa), 25,000 psig (170.1 MPa), 30,000 psig (204.1 MPa), 35,000 psig (238.1 MPa) and 40,000 psig (272.1 MPa). The cell is maintained at each pressure (P) and temperature (T) for around 10 minutes to allow the temperature to stabilize so that the fluctuation of T is less than ± 0.30°C. It should also be noted that the pressure is not increased monotonically, but it is changed randomly from low pressure to high pressure to avoid any systematic error. Therefore, the internal volume of the cell is determined by dividing the mass of the loaded n-decane by the density obtained from the NIST Chemistry Webbook [37] at a given

temperature, pressure, and LVDT reading. The calibration is repeated with a new loading of n-decane at 150°C and 250°C to account for any temperature effects on the cell volume. All of the calibration experiments are performed with the stir bar in the cell.

Figure 5 shows the view cell volume calibration results at 50, 150, and 250°C using n-decane as the working fluid. The n-decane densities at each temperature and pressure are obtained from the NIST Chemistry Webbook [37], which reports an uncertainty of 0.05% between 17 and 47°C, 0.2% at temperatures to 127°C, somewhat higher uncertainties above 100 MPa, up to 0.5%, 1% in the liquid phase up to 500 MPa, and 2% at higher temperatures.

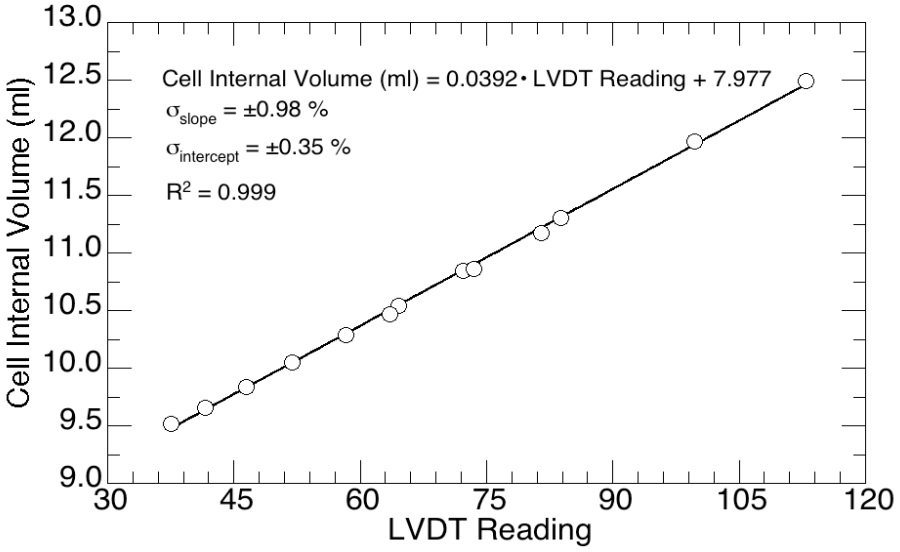

Figure 5. Calibration results for the cell internal volume used in this study at 50, 150, and 250°C using n-decane as the reference fluid. σ_{slope} and $\sigma_{intercept}$ are the uncertainties of the fit of curve to the calibration data.

The calibration curve for the inferred volume is

Cell Internal Volume (ml) = 0.0392 • LVDT Reading + 7.977 (3)

Note that σ_{slope} and $\sigma_{intercept}$ refer to the uncertainties of slope and intercept of the internal cell volume calibration curve, respectively. The small values of the uncertainties of the slope and intercept indicate the accuracy of the slope of the calibration curve. The error bars are also plotted, but they are much smaller than the size of the data points and cannot be seen in the figure.

2.3 Materials

The n-pentane (99.0% purity), n-octane (99.0% purity), cyclooctane (99.0% purity), 2,2,4-trimethylpentane (99.8% purity), n-decane (99.0% purity), and toluene (99.9% purity) were all purchased from Sigma-Aldrich and used without further purification.

2.4 Density Measurement Technique

The experimental procedure for measuring the density is similar to the technique used to calibrate the cell: flush the cell with ethane three times to remove the air inside it, load 7.0 to 9.0 ± 0.001 grams of the testing fluid, increase the pressure in stages to ~40,000 psig, and at each P and T record the LVDT reading. Since the relationship between the internal cell volume and the LVDT reading has been set by the previous calibration step, the density of the fluid loaded into the cell can be obtained by dividing the mass of the fluid by the cell internal volume at a given P and T. All the density measurements are taken with the stir bar in the cell and each density data

point is obtained by randomly changing the system pressure instead of always increasing from low pressure to high pressure to avoid any potential systematic error. The cell is maintained at a given P and T for 10 minutes to ensure that the temperature variation is less than ± 0.30°C. Figure 6 shows the temperature fluctuation with time after increasing the pressure from atmosphere pressure to 4,000 psig at around 150°C for n-pentane. These data show that 10 minutes is time enough for the stabilization of the temperature. Although waiting for a longer time is better for reducing the level of temperature fluctuation, operating at high temperatures for a long period of time may lead to the degradation of the o-rings.

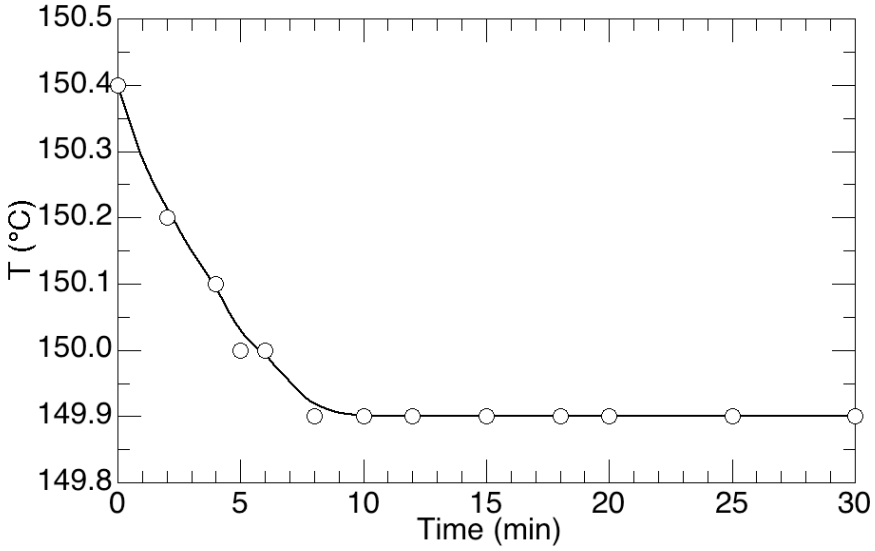

Figure 6. Variation of the cell internal temperature after increasing the pressure from atmospheric pressure to 4,000 psig at ~150°C.

Chapter 3 Results and Discussion

3.1 Experimental Data

The density data for n-pentane, n-octane, cyclooctane, 2,2,4-trimethylpentane (isooctane), n-decane, and toluene are listed in Tables 6 through 11, respectively, at pressure up to ~280 MPa (~40,000 psig) and temperature up to ~250°C. The temperature variation for all 18 isotherms is within ± 0.30°C and the variation for 14 of the isotherms is less than ± 0.20°C. For the remaining four isotherms with temperature variations between ± 0.20 and ± 0.30°C, three of the isotherms are at ~250°C. Hence, this temperature variation at 250°C is not expected to have a significant impact on the quality of these data. Table 12 shows the temperatures and pressures of the density data reported in this study that are not covered in the literature data.

The mean absolute percentage deviation (MAPD) is introduced in these tables to show how much our experimental density data deviates from the literature data. MAPD is defined as

$$\mathrm{MAPD} = \frac{1}{n}\sum_{1}^{n}\left|\frac{\rho_{i,\mathrm{experimental}} - \rho_{i,\mathrm{literature}}}{\rho_{i,\mathrm{experimental}}}\right| \bullet 100 \qquad (4)$$

where n indicates the number of data points, $\rho_{i,\ experimental}$ and $\rho_{i,\ literature}$ refer to a single density obtained in this study and density reported in the literature, respectively. MAPD values are reported in Table 6 through 11 for each working fluid except cyclooctane in Table 9, since, as far as we know, there are no cyclooctane data available on any literature.

Table 6. Density of n-pentane at 52.7, 149.9, and 247.3°C obtained in this study. MAPD is the mean absolute percent deviation in density for n data points relative to those calculated at the NIST web site to a maximum density of 0.762 g/ml or a pressure of 100 MPa [37].

52.7 ± 0.2°C MAPD = 0.5, n = 9		149.9 ± 0.1°C MAPD = 0.5, n = 4		247.3 ± 0.3°C MAPD = 0.5, n = 4	
P (MPa)	Density (g/ml)	P (MPa)	Density (g/ml)	P (MPa)	Density (g/ml)
1.8	0.595	28.6	0.553	28.5	0.472
3.6	0.598	43.7	0.570	43.1	0.507
7.0	0.603	56.8	0.592	54.9	0.526
13.8	0.613	85.5	0.621	87.1	0.562
28.9	0.630	112.8	0.645	112.7	0.584
43.3	0.643	137.0	0.658	141.2	0.603
55.3	0.653	171.9	0.676	174.7	0.622
70.9	0.664	209.4	0.692	209.6	0.639
84.1	0.672	241.0	0.702	241.1	0.652
110.2	0.686	276.6	0.712	273.5	0.665
137.8	0.700				
171.0	0.714				
206.2	0.727				
239.5	0.739				
275.5	0.750				

Table 7. Density of n-octane at 48.7, 150.2, and 248.4°C obtained in this study. MAPD is the mean absolute percent deviation in density for n data points relative to data of Caudwell et al. [28] to a maximum pressure of 200 MPa and a temperature of 200°C and to densities calculated at the NIST web site to a maximum density of 0.764 g/ml or a pressure of 100 MPa [37].

48.7 ± 0.1°C MAPD = 0.5, n = 10		150.2 ± 0.2°C MAPD = 0.5, n = 9		248.4 ± 0.3°C MAPD = 0.3, n = 4	
P (MPa)	Density (g/ml)	P (MPa)	Density (g/ml)	P (MPa)	Density (g/ml)
14.3	0.688	28.7	0.628	15.4	0.538
28.5	0.702	56.1	0.659	28.0	0.571
56.3	0.721	84.2	0.681	55.9	0.614
84.0	0.735	111.2	0.699	82.9	0.636
111.3	0.748	139.0	0.714	112.0	0.655
139.9	0.760	172.9	0.730	140.5	0.672
172.5	0.771	207.5	0.744	174.6	0.689
207.6	0.783	240.6	0.756	208.7	0.704
241.0	0.792	275.7	0.768	242.7	0.718
274.4	0.802			276.9	0.730

Table 8. Density of 2,2,4-trimethylpentane (isooctane) at 50.9, 149.5, and 247.1°C obtained in this study. MAPD is the mean absolute percent deviation in density for n data points relative to data of Malhotra and Woolf [24, 31] for densities to a maximum pressure of 280 MPa at 50.9°C.

50.9 ± 0.1°C MAPD = 0.3, n = 16		149.5 ± 0.1°C No MAPD		247.1 ± 0.2°C No MAPD	
P (MPa)	Density (g/ml)	P (MPa)	Density (g/ml)	P (MPa)	Density (g/ml)
4.2	0.671	28.0	0.621	14.5	0.524
6.5	0.674	55.9	0.660	28.3	0.567
9.1	0.677	83.0	0.684	55.7	0.611
11.5	0.679	110.2	0.701	85.1	0.639
14.4	0.683	137.6	0.717	112.3	0.659
29.1	0.697	172.8	0.735	139.4	0.676
42.3	0.708	206.4	0.750	172.8	0.694
55.7	0.718	240.8	0.764	208.2	0.710
70.8	0.727	275.6	0.776	242.4	0.724
84.3	0.734			276.3	0.736
112.3	0.749				
143.3	0.762				
178.4	0.777				
211.5	0.789				
246.7	0.799				
281.1	0.808				

Table 9. Density of cyclooctane at 51.3, 151.7, and 250.7°C obtained in this study.

51.3 ± 0.1°C No MAPD		151.7 ± 0.2°C No MAPD		250.7 ± 0.1°C No MAPD	
P (MPa)	Density (g/ml)	P (MPa)	Density (g/ml)	P (MPa)	Density (g/ml)
14.0	0.830	28.1	0.745	14.8	0.675
28.8	0.841	55.8	0.777	28.0	0.754
42.9	0.850	84.0	0.798	43.1	0.718
56.4	0.857	111.0	0.814	56.8	0.805
70.8	0.865	138.3	0.828	69.3	0.848
84.5	0.872	172.1	0.844	84.1	0.699
		206.7	0.859	97.0	0.788
		240.5	0.872	111.0	0.742
		274.0	0.885	125.1	0.820
				138.3	0.732
				172.9	0.781
				205.9	0.763
				240.2	0.834
				275.7	0.772

Table 10. Density of n-decane at 51.3, 149.7, and 247.0°C obtained in this study. MAPD is the mean absolute percent deviation in density for n data points relative to data of Caudwell et al. [28] to a maximum pressure of 200 MPa and a temperature of 200°C and to densities calculated at the NIST web site to a maximum density of 0.770 g/ml [37].

51.3 ± 0.2°C MAPD = 0.8, n = 7		149.7 ± 0.3°C MAPD = 0.1, n = 8		247.0 ± 0.3°C MAPD = 0.2, n = 10	
P (MPa)	Density (g/ml)	P (MPa)	Density (g/ml)	P (MPa)	Density (g/ml)
14.6	0.714	15.0	0.648	15.3	0.580
29.3	0.724	28.0	0.667	28.4	0.605
56.6	0.741	56.8	0.692	55.5	0.639
82.7	0.754	83.1	0.710	85.7	0.666
111.4	0.767	113.5	0.727	112.8	0.685
144.2	0.780	141.9	0.741	140.5	0.701
173.2	0.790	174.9	0.756	174.5	0.719
207.0	0.801	204.8	0.767	209.5	0.734
241.2	0.811			245.4	0.749
274.5	0.820			278.8	0.762

Table 11. Density of toluene at 49.7, 149.1, and 251.9°C obtained in this study. MAPD is the mean absolute percent deviation in density for n data points relative to densities calculated at the NIST web site to a maximum density of 0.975 g/ml [37].

49.7 ± 0.1°C MAPD = 0.4, n = 8		149.1 ± 0.2°C MAPD = 0.7, n = 9		251.9 ± 0.1°C MAPD = 0.4, n = 9	
P (MPa)	Density (g/ml)	P (MPa)	Density (g/ml)	P (MPa)	Density (g/ml)
54.1	0.882	28.6	0.780	39.6	0.713
83.2	0.899	55.5	0.811	56.3	0.738
110.8	0.912	82.5	0.836	82.7	0.767
137.8	0.925	109.6	0.857	109.8	0.791
172.2	0.937	137.9	0.872	137.7	0.811
206.7	0.952	173.4	0.887	173.5	0.836
239.6	0.961	206.5	0.899	204.8	0.849
274.9	0.973	240.3	0.913	239.5	0.865
		274.6	0.928	274.4	0.881

Table 12. The approximate temperatures and pressures of the density data reported in this study that are not covered in the literature data.

Reference	Pressure (MPa) Min	Pressure (MPa) Max	Temperature (°C) Min	Temperature (°C) Max	Temperatures and Pressures for Density Data Obtained in the Present Study that Differ From Available Reference Data
			n-Pentane		
Bridgman (1931)[20]	98.1	981	0	95	150°C: P (MPa) < 280 250°C: P (MPa) < 280
Byun (2000)[9]	7.0	241	50	150	50°C: 241 < P (MPa) < 280 150°C: 241 < P (MPa) < 280 250°C: P (MPa) < 280
Easteal (1987)[29]	0.1	60	5	65	50°C: 60 < P (MPa) < 280 150°C: P (MPa) < 280 250°C: P (MPa) < 280
Audonnet (2001)[4]	0.1	100	30	110	50°C: 100 < P (MPa) < 280 150°C: P (MPa) < 280 250°C: P (MPa) < 280
Oliveira (1992)[23]	0.1	252	30	50	50°C: 252 < P (MPa) < 280 150°C: P (MPa) < 280 250°C: P (MPa) < 280
Palavra (1987)[21]	1.8	283	33	69	150°C: P (MPa) < 280 250°C: P (MPa) < 280
Kiran (1992)[10]	7.5	70	45	170	50°C: 70 < P (MPa) < 280 150°C: 70 < P (MPa) < 280 250°C: P (MPa) < 280
Kiran (1996)[30]	8.1	65	75	150	50°C: 65 < P (MPa) < 280 150°C: 65 < P (MPa) < 280 250°C: P (MPa) < 280

Table 12. Continued

Reference	Pressure (MPa) Min	Pressure (MPa) Max	Temperature (°C) Min	Temperature (°C) Max	Temperatures and Pressures for Density Data Obtained in the Present Study that Differ From Available Reference Data
			n-Octane		
Bridgman (1931)[20]	49.0	981	0	95	150°C: P (MPa) < 280 250°C: P (MPa) < 280
Harris (1997)[22]	0.1	373	10	80	150°C: P (MPa) < 280 250°C: P (MPa) < 280
Caudwell (2009)[28]	0.1	202	25	200	50°C: 202 < P (MPa) < 280 150°C: 202 < P (MPa) < 280 250°C: P (MPa) < 280
Oliveira (1992)[23]	0.1	253	30	75	50°C: 253 < P (MPa) < 280 150°C: P (MPa) < 280 250°C: P (MPa) < 280
Kiran (1992)[10]	8.0	66	50	175	50°C: 66 < P (MPa) < 280 150°C: 66 < P (MPa) < 280 250°C: P (MPa) < 280
Moravkova (2006)[15]	0.1	40	25	55	50°C: 40 < P (MPa) < 280 150°C: P (MPa) < 280 250°C: P (MPa) < 280
Dymond (1982)[25]	0.1	480	25	75	150°C: P (MPa) < 280 250°C: P (MPa) < 280

Table 12. Continued

Reference	Pressure (MPa) Min	Pressure (MPa) Max	Temperature (°C) Min	Temperature (°C) Max	Temperatures and Pressures for Density Data Obtained in the Present Study that Differ From Available Reference Data
2,2,4-Trimethylpentane					
Malhotra (1990)[31]	49.0	588	5	65	150°C: P (MPa) < 280 250°C: P (MPa) < 280
Malhotra (1993)[24]	0.1	374	40	80	150°C: P (MPa) < 280 250°C: P (MPa) < 280
Padua (1994)[32]	0.1	100	25	75	50°C: 100 < P (MPa) < 280 150°C: P (MPa) < 280 250°C: P (MPa) < 280
Padua (1996)[5]	0.1	100	-75	75	50°C: 100 < P (MPa) < 280 150°C: P (MPa) < 280 250°C: P (MPa) < 280
n-Decane					
Bridgman (1931)[20]	49.0	785	0	95	150°C: P (MPa) < 205 250°C: P (MPa) < 280
Audonnet (2004)[33]	0.1	76	30	120	50°C: 76 < P (MPa) < 275 150°C: P (MPa) < 205 250°C: P (MPa) < 280
Caudwell (2009)[28]	0.1	192	25	100	50°C: 192 < P (MPa) < 275 150°C: P (MPa) < 205 250°C: P (MPa) < 280
Oliveira (1992)[23]	0.1	254	30	75	50°C: 254 < P (MPa) < 275 150°C: P (MPa) < 205 250°C: P (MPa) < 280
Dymond (1982)[25]	0.1	420	25	100	150°C: 54 < P (MPa) < 205 250°C: P (MPa) < 280

Table 12. Continued

Reference	Pressure (MPa) Min	Pressure (MPa) Max	Temperature (°C) Min	Temperature (°C) Max	Temperatures and Pressures for Density Data Obtained in the Present Study that Differ From Available Reference Data
			Toluene		
Harris (1997)[22]	0.1	373	25	50	150°C: P (MPa) < 275 250°C: P (MPa) < 275
Oliveira (1992)[23]	0.1	252	30	75	50°C: 252 < P (MPa) < 275 150°C: P (MPa) < 275 250°C: P (MPa) < 275
Assael (1991)[34]	0.1	71	30	50	50°C: 71 < P (MPa) < 275 150°C: P (MPa) < 275 250°C: P (MPa) < 275
Et-Tahir (1995)[16]	0.1	40	25	90	50°C: 40 < P (MPa) < 275 150°C: P (MPa) < 275 250°C: P (MPa) < 275
Glen (2009)[35]	0.6	30	20	100	50°C: 30 < P (MPa) < 275 150°C: P (MPa) < 275 250°C: P (MPa) < 275
Dymond (1995)[36]	0.1	492	25	50	150°C: P (MPa) < 275 250°C: P (MPa) < 275
Polhler (1996)[11]	3.4	65	50	150	50°C: 65 < P (MPa) < 275 150°C: 65 < P (MPa) < 275 250°C: P (MPa) < 275

Among all theses data, it should be noted that the cyclooctane density data at 50°C is only measured up to ~90 MPa (see Table 9), above which it reaches a point where the liquid phase

solidifies. In the case of 150 and 250°C, the liquid-to-solid transition is not observed up to ~275 MPa.

A comparison of the temperatures and pressures in this study with those from previous studies (see Table 1) show that our data extend the current density database to higher temperatures and/or pressures. We also report the cyclooctane densities, which are not reported in the literature. Detailed comparisons of the experimental data from the present study with the literature is presented in Section 3.3.

Our collaborators at the University of Pittsburgh used our data to test the performance of several different equations of state (EOS) to predict fluid densities. They found the statistical associating fluid theory, or SAFT, EOS provided relatively accurate density predictions over a wide range of temperatures and pressures. For example, comparing the calculated densities using Peng-Robinson EOS (shown in Figure 7) and calculated densities using PC-SAFT EOS (shown in Figure 8), the PC-SAFT EOS predict the densities much better than Peng-Robinson EOS in the full range of pressures and temperatures. Therefore, for the other hydrocarbons, the calculated densities using PC-SAFT EOS are only shown. The SAFT EOS is a perturbation equation in that the fluid is first considered as a mixture of unconnected hard spheres that exhibit attractive dispersion forces. A chain connectivity term is then employed to account for the bonding of these spheres to form longer molecules or polymers. An association term can then be incorporated to account for hydrogen bonding associations. With the SAFT EOS each molecule is characterized by a segment size, a number of segments in the molecule, a segment–segment dispersion energy and an association energy and volume if the molecule can self- or cross-associate. Each term of

the SAFT EOS has been tested against molecular simulations. Each of the five parameters for associating molecules has a physical meaning, and each term of the SAFT EOS can be refined or modified. A notable example of such a modification is the perturbed chain SAFT (PC-SAFT) EOS, in which the segment term that accounts for attractive (dispersion) van der Waal forces are considered. In PC-SAFT the Barker-Henderson second-order perturbation theory of spherical molecules is applied to chain molecules rather than segments as in SAFT, resulting in the modeling of dispersion interactions as occurring between chains.

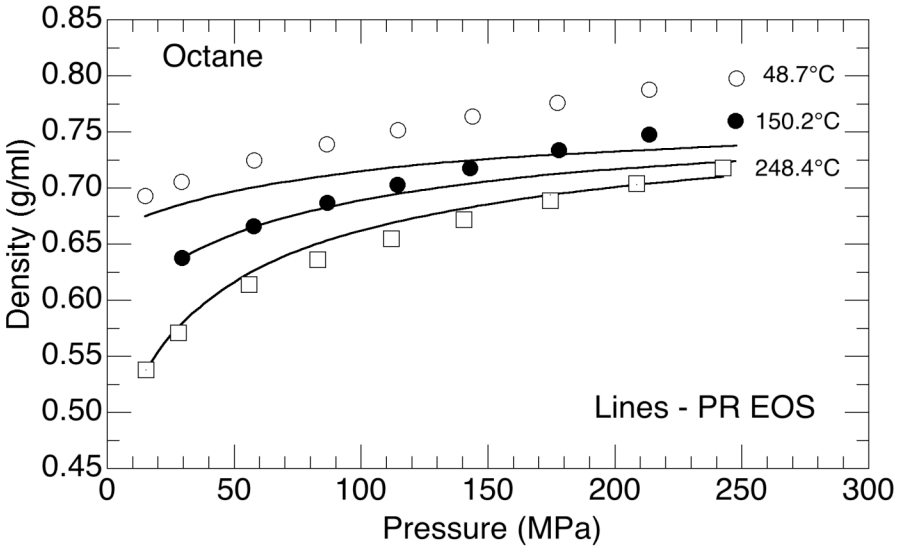

Figure 7. High-pressure n-octane density data at 48.7, 150.2, and 248.4°C obtained in this study. The lines represent the calculated densities using the Peng-Robinson equation of state.

Figures 9 and Figure 10 show experimental density data for 2,2,4-trimethylpentane and cyclooctane measured in this study along with the density calculated by the PC-SAFT equation done at the University of Pittsburgh.

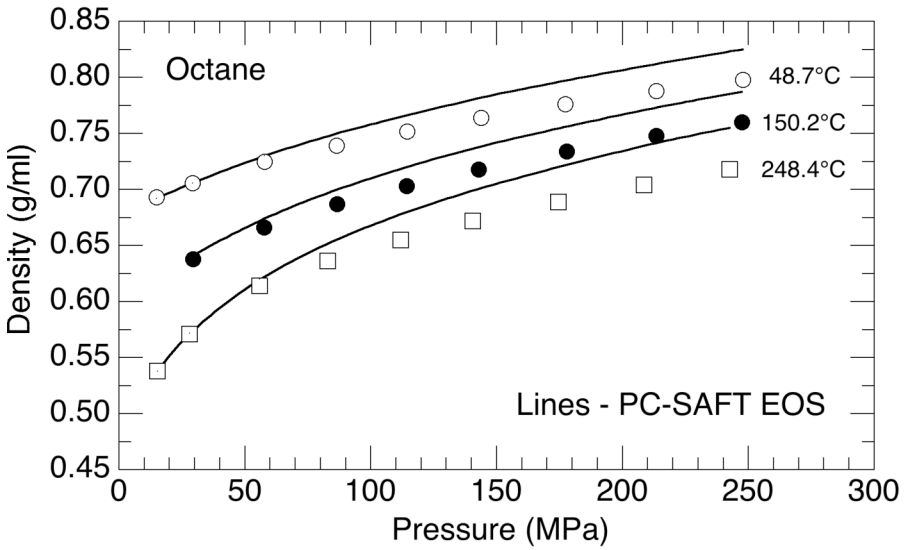

Figure 8. High-pressure n-octane density data at 48.7, 150.2, and 248.4°C obtained in this study. The lines represent the calculated densities using the PC-SAFT equation of state.

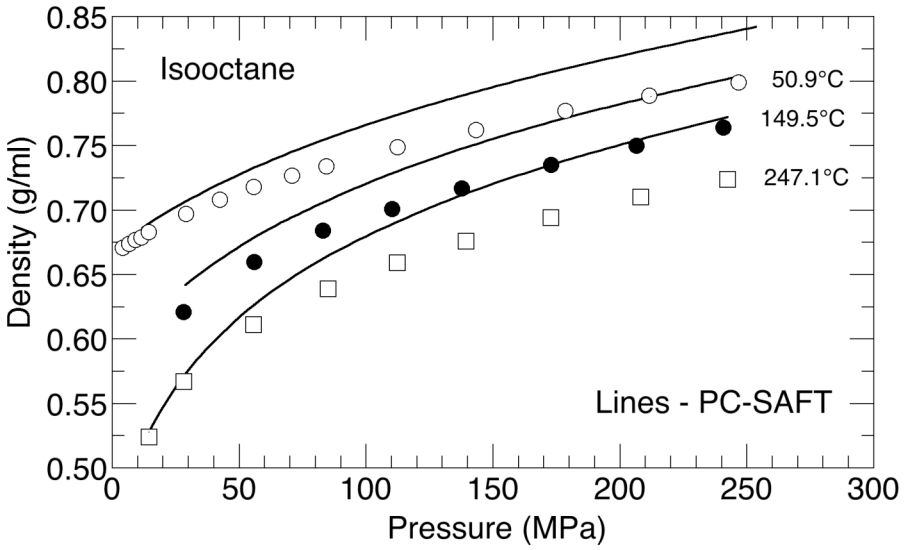

Figure 9. High-pressure 2,2,4-trimethylpentane (isooctane) density data at 50.9, 149.5, and 247.1°C obtained in this study. The lines represent the calculated densities using the PC-SAFT equation of state.

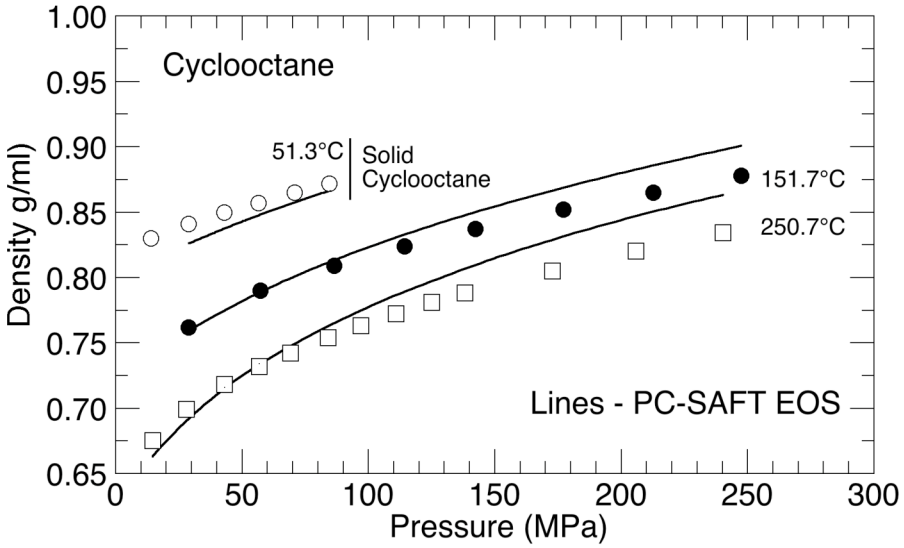

Figure 10. High-pressure cyclooctane density data at 51.3, 151.7, and 250.7°C obtained in this study. The lines represent the calculated densities using the PC-SAFT equation of state.

As can be seen in the figures, the PC-SAFT modeling results are reasonably accurate at low pressures. The modeling curves at each temperature are almost parallel and do not cross one another, indicating thermodynamic consistency. Although the calculated densities deviate from the experimental data at pressures above 150 MPa, it should be noted that the PC-SAFT EOS parameter values for the components considered in this study are taken directly from the literature and no attempt is made to optimize these parameters further. In the future, more work will be done by our research group to improve the PC-SAFT EOS, especially the optimization of the parameters.

3.2 Error Analysis of Density Measurement

The purpose of this section is to estimate the errors in the density experiments. We expect the errors to be in the thermocouple, pressure transducer, LVDT, and the weighing scale. The errors may also result from the view cell volume calibration process and the calculated reference density obtained from the NIST Density Webbook [37].

Since the density is equal to the mass loaded into the cell divided by the volume at a given P and T, the uncertainty of the calculated density can be estimated as

$$\sigma_\rho = \sqrt{\left(\frac{\partial \rho}{\partial m}\right)^2 \bullet \sigma_m^2 + \left(\frac{\partial \rho}{\partial V}\right)^2 \bullet \sigma_V^2} \qquad (5)$$

where ρ, m, and V represent the density, mass, and volume of the working fluid and σ_ρ, σ_m, and σ_V are the uncertainty of the density, mass, and volume, respectively.

By substituting for the partial derivative terms in Equation (5), we get

$$\sigma_\rho = \sqrt{\left(\frac{1}{V}\right)^2 \bullet \sigma_m^2 + \left(\frac{m}{V^2}\right)^2 \bullet \sigma_V^2} \qquad (6)$$

σ_m comes from the accuracy of the weighing scale, which is 0.001 g. Since the volume of the fluid at a given P and T is obtained from the cell volume calibration using n-decane as the reference fluid, σ_V is estimated from the equation $V_{C10} = \frac{m_{C10}}{\rho_{C10}}$ as follows

$$\sigma_{V_{C10}} = \sqrt{\left(\frac{\partial V_{C10}}{\partial \rho_{C10}}\right)^2 \bullet \sigma_{m_{C10}}^2 + \left(\frac{\partial V_{C10}}{\partial \rho_{C10}}\right)^2 \bullet \sigma_{\rho_{C10}}^2} \quad (7)$$

where the subscript C10 indicates n-decane.

Again, the following Equation (8) is obtained by substituting for the partial derivative terms in Equation (7)

$$\sigma_{V_{C10}} = \sqrt{\left(\frac{1}{\rho_{C10}}\right)^2 \bullet \sigma_{m_{C10}}{}^2 + \left(\frac{m_{C10}}{\rho_{C10}{}^2}\right)^2 \bullet \sigma_{\rho_{C10}}{}^2} \quad (8)$$

Density data for the reference fluid, n-decane, at different pressures and temperatures are obtained from the NIST website [37], which shows that the uncertainties in the density of the liquid phase are 0.2% at temperatures to 127°C (with somewhat higher uncertainties above 100 MPa, up to 0.5%), 1% in the liquid phase up to 500 MPa, and 2% at higher temperatures.

Equation (6) is used to estimate σ_ρ. Here an example set of calculations are presented to estimate the expected largest percent error in the experimental density data from this study. To obtain a maximum value of σ_{VC10}, the value of ρ_{C10} should be small and the value of m_{C10} should be large. The smallest value of ρ_{C10} is obtained at the highest temperature at ambient pressure. Since n-decane at 250°C at ambient pressure is the vapor phase instead of liquid phase, we use the density, 0.524 g/ml, at ~0.5 MPa, which is the lowest pressure n-decane maintains a liquid phase at 250°C. The largest value of m_{C10} refers to the biggest loading of working fluid, which is

typically nine grams. As previously mentioned, σ_{mC10} equals 0.001 g and, therefore, the maximum value of σ_{VC10} from Equation (8) is 0.0343 ml. Employing this value of σ_V into Equation (6) and using the smallest cell internal volume of 8.5 ml, the maximum uncertainty in density, σ_ρ is 0.0043 g/ml. Therefore, the estimate of the accumulated error of the experimental density data is less than 0.82 %.

3.3 Tait Equation

The experimental data at low pressure and temperature are compared with a limited set of data obtained from the NIST web site [37] and other literature studies. Since temperatures and pressures in these researches are slightly different from the conditions in this study, an equation is required to correlate them to make all of the data comparable to each other. Such an equation is the so-called "Tait Equation".

Today, the Tait equation is widely accepted as a common method to correlate liquid density data over a broad pressure and temperature range. The original equation was suggested by Peter Guthrie Tait in 1888 to show the relation between pressure and average compressibility of the fluid when he found "the average compressibility through any range of pressure falls off more and more slowly as the range is greater" [38]. This equation is in good agreement with the experimental data for solids up to a few gigapascals of pressure, while it does not work quite well for liquids at extremely high pressure. For example, in the case of organic liquids, it only matches the experimental data up to 150 MPa [38]. Therefore, a modified Tait equation was

suggested to correlate the density of liquids and liquid mixtures over much wider range of pressures

$$\frac{\rho - \rho_0}{\rho} = C \log_{10} \frac{P + B}{P_0 + B} \tag{9}$$

or the equivalent expression in terms of volume

$$\frac{V_0 - V}{V_0} = C \bullet \log_{10} \frac{P + B}{P_0 + B} \tag{10}$$

where P_0 = 0.1 MPa, ρ_0 or V_0 is the density or volume when $P = P_0$, and B and C are parameters that can be obtained from a fit of available data. When it comes to organic liquids, C is a temperature independent constant while B decreases when temperature goes higher. Furthermore, it is found that the value of parameter C is usually between 0.20 and 0.21 for n-alkane hydrocarbons [39].

In this study, the modified Tait equation is employed for the reference data to correlate them with our experimental data. ρ_0 and B are expressed as a function of temperature (T) as follows

$$\rho_0 = \sum_i^2 a_i T^i \tag{11}$$

$$B = \sum_i^2 b_i T^i \tag{12}$$

where a_i and b_i are coefficients. The units of ρ_0, T, and B are kg/m^3, K, and MPa, respectively.

Through the above approach, literature data with different conditions are recalculated to match the P and T of our experimental data at given temperatures and pressures. Figures 10 through 12 shows the percent deviation of our n-octane, 2,2,4-trimethylpentane, and n-decane density data from the literature data at each pressure at around 50°C for all the testing fluids. As can be seen in these figures, all the data points are within the estimated accumulate error, ±0.82 %.

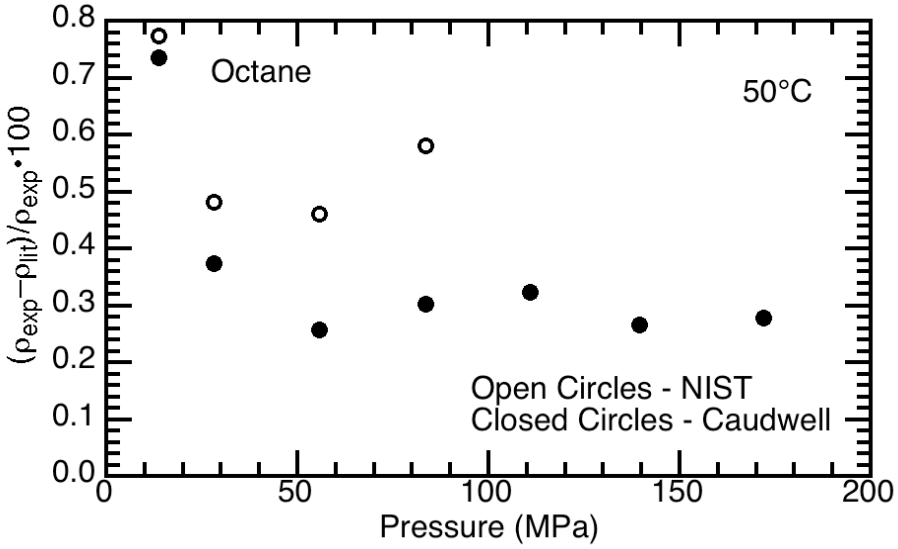

Figure 11. Percent deviation of the 50°C experimental n-octane density data from densities calculated at the NIST web site [37] and the data of Caudwell et al. [28].

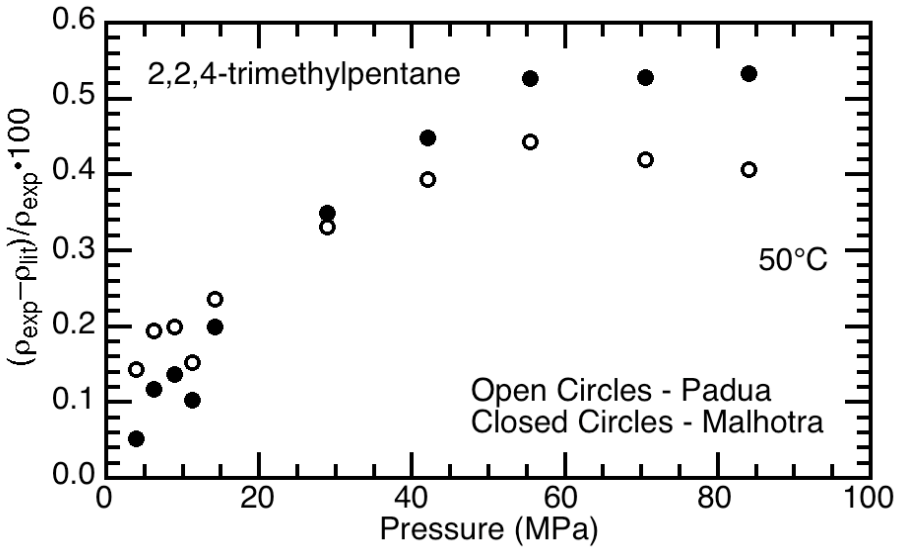

Figure 12. Percent deviation of the 50°C experimental 2,2,4-trimethylpentane (isooctane) density data from the data of Padua et al. [3, 5] and Malhotra et al. [24, 31].

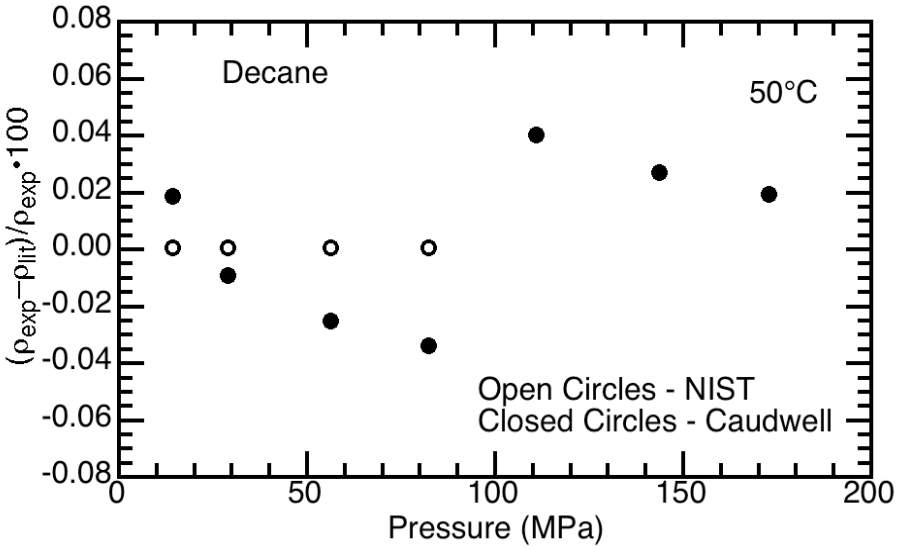

Figure 13. Percent deviation of the 50°C experimental n-decane density data from densities calculated at the NIST web site [37] and the data of Caudwell et al. [28].

We also calculate the deviation at each pressure for the other hydrocarbons at approximately 50°C and for all of the hydrocarbons, except cyclooctane, at approximately 150°C and 250°C, both of which are not shown in Figures 10-12. The deviation for each isotherm is within the estimated accumulated error of 0.82 %.

The mean absolute percentage deviation (MAPD) is then employed to show the extent that our experimental density data deviates from the literature data. For the 35 n-pentane density data points obtained in this study, the first nine density values at 52.7°C and the first four values at 149.9 and at 247.3°C are directly comparable to those obtained from the NIST web site [37]. The nine data points at 52.7°C have an MAPD of 0.1% and the four data points at 149.9 and at 247.3°C have an MAPD of 0.5%, which is shown in Table 6. These MAPD values are well within the estimated accumulated error of 0.82 % for the experimental densities reported here. The n-pentane density data of Easteal and Woolf at 50.0°C [29] are within 0.5% of those obtained by calculation from the NIST web site at pressures to 100 MPa and, therefore, the first nine density values at 52.7°C in the present study also agree with those of Easteal and Woolf to within 0.5%. The first four density data points at 250°C also have an MAPD of 0.5% relative to those obtained from the NIST web site.

Table 7 shows that all of the n-octane data at 48.7°C and at 150.2°C each have an MAPD of 0.5%, both relative to the data of NIST web site [37] and Caudwell et al. [28]. Since the data by Caudwell et al. are within ±0.3 % of the data from Dymond et al. [25] and Bridgman [20], our data also agree with these literature data within our estimated accumulate error, 0.82 %. The first four n-octane density values at 248.4°C have an MAPD of 0.3% relative to the values obtained by

calculation from the NIST web site [37] that are limited to a maximum density of 0.764 g/ml or a pressure of 100 MPa. Besides the good agreement with the literature data, there are still two points we are concerned about. As can be observed from Figure 10, the deviation of our n-octane data from literature data at low pressure is much larger than the deviations at other conditions. Note that our data are always a little higher than the literature data, although the reason for this behavior is not apparent.

For the 2,2,4-trimethylpentane (isooctane) data shown in Table 8, the MAPD at 50.9°C is within 0.3% relative to the data of Malhotra and Woolf [24, 31] and the data of Padua et al. [3, 5]. Malhotra and Woolf measured isooctane densities using a bellows volumometer to temperatures of 80°C and pressures of 375 MPa and they report an estimated accuracy in density measurements of less than 0.15%. Padua et al. measured isooctane densities using a vibrating-wire densimeter to temperatures of 50°C and pressures of 100 MPa and they report an estimated accuracy in density measurements of ±0.03%. The isooctane data of Padua et al. agree with those of Malhotra and Woolf to within ±0.15% at 50°C [5]. Unfortunately there are no isooctane data available at higher temperatures, however, following the suggestion of Malhotra and Woolf [31] the Tait equation was used to calculate isooctane densities at 149.5°C and pressures to 276 MPa. The MAPD for the isooctane data in the present study at 149.5°C is 0.4% relative to these calculated densities.

To the best of our knowledge there are no cyclooctane data available in the literature so MAPD values are not reported in Table 9. It is not surprising that the cyclooctane densities are much higher than those of octane at similar temperatures and pressures given that cyclooctane, a saturated cyclic hydrocarbon, has a more compact, regular structure.

As is shown in Table 10, the MAPD of n-decane is 0.02% at 51.3°C relative to data of Caudwell et al. [28] who report an accuracy of ± 0.2% at pressures to 200 MPa and temperatures to 100°C, 0.01% at 149.7°C and 247.0°C relative to values obtained by calculation from the NIST web site [37], which are limited to a maximum density of 0.770 g/ml. It is not surprising that our data are so much close to the literature data, since the NIST data are employed to calibrate the cell internal volume. The data of Caudwell et al. for the n-decane are in good agreement with the data of Bridgman [20], Dymond et al. [25], Gehrig and Lentz [12], and Audonnet and Padua [33] and, by inference, our data for n-decane are within ± 0.5 % of the data reported by these authors.

The MAPD of toluene at 49.7°C is 0.4%, at 149.1°C it is 0.7%, and at 215.9°C it is 0.4%, shown in Table 11, relative to values obtained by calculation from the NIST web site [37], which are limited to a maximum density of 0.975 g/ml. The toluene density data reported here have an estimated accumulated error similar to the maximum error reported by Franck et al. [13]. The toluene data in the present study also agree with those of Franck et al. with an MAPD of less than 0.5%.

Chapter 4 Conclusions and Future Work

In this study, the high-pressure view cell system is calibrated for the measurement of fluid densities at different pressures and temperatures. Six hydrocarbons, including n-pentane, n-octane, 2,2,4-trimethylpentane, cyclooctane, n-decane, and toluene are investigated and the density database for these hydrocarbons is extended to ~280 MPa and ~250°C. The mean absolute percent deviation (MAPD) of the experimental data obtained in this study is less than 0.8 % from the literature data, which is within the estimated accumulated error of the view cell system.

There is still some work that should be done in the future, shown as follows.

1. Maintain a more stable temperature during the experiment. In this study, the temperature fluctuation is within ± 0.3°C, which will lead to at most 0.02 % density deviation. Future work will focus on reducing the temperature fluctuation to ± 0.1°C, which only results in at most 0.008% deviation.

2. Measure the densities of mixtures of hydrocarbons. This study only considered the densities of some pure hydrocarbons. In the future, the densities of hydrocarbon mixtures will be obtained to better simulate the densities of multicomponent petroleum liquids.

3. Improve the density model to better predict the densities of pure hydrocarbons or hydrocarbon mixtures at high pressures and temperatures. This study shows the density modeling by the PC-SAFT equation used by our collaborators at the University of Pittsburgh. The calculated densities are in reasonable agreement with experimental data but not so accurate at high pressures. Further work is needed to optimize the parameters of the modeling equation to better fit the experimental data.

List of References

1. Song, C. S., An overview of new approaches to deep desulfurization for ultra-clean gasoline, diesel fuel and jet fuel. *Catalysis Today* **2003,** 86, 211-263.

2. Kagami, N.; Iwamoto, R.; Tani, T., Application of datamining method (ID3) to data analysis for ultra deep hydrodesulfurization of straight-run light gas oil - determination of effective factor of the feed properties to reaction rate of HDS. *Fuel* **2005,** 84, 279-285.

3. Padua, A. A. H.; Fareleira, J. M. N. A.; Calado, J. C. G.; Wakeham, W. A., Validation of an accurate vibrating-wire densimeter: Density and viscosity of liquids over wide ranges of temperature and pressure. *International Journal of Thermophysics* **1996,** 17, 781-802.

4. Audonnet, F.; Padua, A. A. H., Simultaneous measurement of density and viscosity of n-pentane from 298 to 383 K and up to 100 MPa using a vibrating-wire instrument. *Fluid Phase Equilibria* **2001,** 181, 147–161.

5. Padua, A. A. H.; Fareleira, J. M. N. A.; Calado, J. C. G.; Wakeham, W. A., Density and viscosity measurements of 2,2,4-trimethylpentane (isooctane) from 198 K to 348 K and up to 100 MPa. *Journal of Chemical and Engineering Data* **1996,** 41, 1488-1494.

6. Padua, A. A. H.; Fareleira, J.; Calado, J. C. G.; Wakeham, W. A., Electromechanical model for vibrating-wire instruments. *Review of Scientific Instruments* **1998,** 69, 2392-2399.

7. Caudwell, D. R.; Trusler, J. P. M.; Vesovic, V.; Wakeham, W. A., The viscosity and density of n-dodecane and n-octadecane at pressures up to 200 MPa and temperatures up to 473 K. *International Journal of Thermophysics* **2004,** 25, 1339-1352.

8. Beck, P. J.; Easteal, A. J.; Hurle, R. L.; Woolf, L. A., High-precision measurements with a bellows volumometer. *Journal of Physics E: Scientific Instruments* **1982,** 15, 360-363.

9. Byun, H. S.; DiNoia, T. P.; McHugh, M. A., High pressure density of ethane, pentane, deuterated pentane, 25.5 wt% ethane in deuterated pentane, 2.4 wt% deuterated poly(ethylene-co-butene) (PEB) in ethane, 5.3 wt% hydrogenated PEB in pentane, 5.1 wt% hydrogenated PEB

in deuterated pentane, and 4.9 wt% hydrogenated PEB in deuterated pentane + 23.1 wt% ethane. *Journal of Chemical and Engineering Data* **2000,** 45, 810-814.

10. Kiran, E.; Sen, Y. L., High-pressure viscosity and density of n-alkanes. *International Journal of Thermophysics* **1992,** 13, 411-442.

11. Pölhler, H.; Kiran, E., Volumetric properties of carbon dioxide + toluene at high pressures. *Journal of Chemical and Engineering Data* **1996,** 41, 482-486.

12. Gehrig, M.; Lentz, H., Values of p(V,T) for n-decane up to 300 MPa and 673 K. *Journal of Chemical Thermodynamics* **1983,** 15, 1159-1167.

13. Franck, E. U.; Kerschbaum, S.; Wiegand, G., The density of toluene at high pressures to 673 K and 300 MPa. *Berichte Bunsenges Gesellschaft Physical Chemistry* **1998,** 102, 1794-1797.

14. Lentz, H., A method of studying the behavior of fluid phases at high pressures and temperatures. *Review of Scientific Instruments* **1969,** 40, 371-372.

15. Moravkova, L.; Wagner, Z.; Aim, K.; Linek, J., (P,Vm,T) measurements of (octane + 1-chlorohexane) at temperatures from 298.15 K to 328.15 K and at pressures up to 40 MPa. *Journal of Chemical Thermodynamics* **2006,** 38, 861–870.

16. Et-Tahir, A.; Boned, C.; Lagourette, B.; Xans, P., Determination of the viscosity of various hydrocarbons and mixtures of hydrocarbons versus temperature and pressure. *International Journal of Thermophysics* **1995,** 16, 1309-1334.

17. Lagourette, B.; Boned, C.; Saintguirons, H.; Xans, P.; Zhou, H., Densimeter calibration method versus temperature and pressure. *Measurement Science & Technology* **1992,** 3, 699-703.

18. Zeberg-Mikkelsen, C. K.; Barrouhou, M.; Baylaucq, A.; Boned, C., Viscosity and density measurements of binary mixtures composed of methylcyclohexane plus cis-decalin versus temperature and pressure. *International Journal of Thermophysics* **2003,** 24, 361-374.

19. Boned, C.; Zeberg-Mikkelsen, C. K.; Baylaucq, A.; Dauge, P., High-pressure dynamic viscosity and density of two synthetic hydrocarbon mixtures representative of some heavy petroleum distillation cuts. *Fluid Phase Equilibria* **2003,** 212, 143-164.

20. Bridgman, P. W., The volume of eighteen liquids as a function of pressure and temperature. *Proceedings of the American Academy of Arts and Sciences* **1931,** 66, 185-233.

21. Palavra, M. F.; Wakeham, W. A.; Zalaf, M., Thermal conductivity of normal pentane in the temperature range 306-360 K at pressures up to 0.5 GPa. *International Journal of Thermophysics* **1987,** 8, 305-318.

22. Harris, K. R.; Malhotra, R.; Woolf, L. A., Temperature and density dependence of the viscosity of octane and toluene. *Journal of Chemical and Engineering Data* **1997,** 42, 1254-1260.

23. Oliveira, C. M. B. P.; Wakeham, W. A., The viscosity of five liquid hydrocarbons at pressures up to 250 MPa. *International Journal of Thermophysics* **1992,** 13, 773-790.

24. Malhotra, R.; Woolf, L. A., Volumetric measurements under pressure for 2.2.4-trimethylpentane at temperatures up to 353.15 K and for benzene and three of their mixtures at temperatures up to 348.15 K. *International Journal of Thermophysics* **1993,** 14, 1153-1172.

25. Dymond, J. H.; Robertson, J.; Isdale, J. D., (p, p, T) of some pure n-alkanes and binary mixtures of n-alkanes in the range 298 to 373 K and 0.1 to 500 MPa. *Journal of Chemical Thermodynamics* **1982,** 20, 305-314.

26. Lee, A.; Ellington, R. T., Viscosity of n-pentane. *Journal of Chemical and Engineering Data* **1965,** 10, 101-104.

27. Lee, A.; Ellington, R. T., Viscosity of n-decane in the liquid phase. *Journal of Chemical and Engineering Data* **1965,** 10, 346-348.

28. Caudwell, D. R.; Treulser, J. P. M.; Vesovic, V.; Wakeham, W. A., Viscosity and density of five hydrocarbon liquids at pressures up to 200 MPa and temperatures up to 473 K. *Journal of Chemical and Engineering Data* **2009,** 54, 359-366.

29. Easteal, A. J.; Woolf, L. A., Volume ratios for n-pentane in the temperature range 278-338 K and at pressures up to 280 MPa. *International Journal of Thermophysics* **1987,** 8, 231-238.

30. Kiran, E.; Pohler, H.; Xiong, Y., Volumetric properties of pentane plus carbon dioxide at high pressures. *Journal of Chemical and Engineering Data* **1996,** 41, 158-165.

31. Malhotra, R.; Woolf, L. A., Thermodynamic properties of 2.2.4-trimethylpentane. *International Journal of Thermophysics* **1990,** 11, 1153-1172.

32. Padua, A. A. H.; Fareleira, J.; Calado, J. C. G.; Wakeham, W. A., A Vibrating-wire densimeter for liquids at high-pressures - the density of 2,2,4-trimethylpentane from 298.15 to 348.15 K and up to 100 MPa. *International Journal of Thermophysics* **1994,** 15, 229-243.

33. Audonnet, F.; Padua, A. A. H., Viscosity and density of mixtures of methane and n-decane from 298 to 393 K and up to 75 MPa. *Fluid Phase Equilibria* **2004,** 216, 235-244.

34. Assael, M. J.; Papadaki, M.; Wakeham, W. A., Measurements of the viscosity of benzene, toluene, and m-xylene at pressure up to 80 MPa. *International Journal of Thermophysics* **1991,** 12, 449-457.

35. Glen, N. F.; Johns, A. I., Determination of the density of toluene in the range from (293 to 373) K and from (0.1 to 30) MPa. *Journal of Chemical and Engineering Data* **2009,** 54, 2538-2545.

36. Dymond, J. H.; Glen, N. F.; Isdale, J. D.; Pyda, M., The viscosity of liquid toluene at elevated pressures. *International Journal of Thermophysics* **1995,** 16, 877-882.

37. NIST thermophysical properties of fluid systems. http://webbook.nist.gov/chemistry/fluid/.

38. Dymond, J. H.; Malhotra, R., The Tait Equation - 100 Years On. *International Journal of Thermophysics* **1988,** 9, 941-951.

39. Dymond, J. H.; Malhotra, R., Densities of n-alkanes and their mixtures at elevated pressures. *International Journal of Thermophysics* **1987,** 8, 541-555.

VITA

Yue Wu was born in August 1986, in Anhui Province of China, and is a Chinese citizen. He received his bachelor degree from Jinan University, Guangzhou, Guangdong Province of China in 2004.